

Dynamics of Viscous Phantom Universe

Ji-Yao Wang,^{1,*} Chao-Jun Feng,^{1,†} Xiang-Hua Zhai,^{1,‡} and Xin-Zhou Li^{1,§}

¹*Division of Mathematical and Theoretical Physics,
Shanghai Normal University, 100 Guilin Road, Shanghai 200234, P.R.China*

The phantom dark energy remarkably boosts our prehension of the accerlerating Universe. In the phantom Universe without bulk viscosity, the models are warmly discussed. In order to generalize the model, we should study it further by considering viscous fluid in the Universe. In this paper, we investigate a class of phantom dark energy models with bulk viscosity by the method of dynamical analysis technique. We show that there are different cosmic late-time behavior and the stability also brings some constraints on the models. We also show that the viscous phantom Universe admit the tracking attractor solution. We find that the viscosity play an important role in the evolution of Universe, the viscosity is big enough, the late time transition from matter dominated to phantom dominated would be different from that of the phantom Universe without viscosity.

PACS numbers:

I. INTRODUCTION

In the past 20 years, the cosmological observational data made it possible to determine the geometry and the expansion history of the Universe [1–7]. The late time acceleration of the Universe indicates that the requiem of either the modification of theories of gravitation or the existence of a component in the Universe that acts as gravitational repulsion. Such a component, that should be relatively uniform in the observable Universe, is called dark energy, whose physical origin is still an open question in modern cosmology. Dark energy is usually described by the equation of state (EoS) $w = p/\rho$, where p is the pressure and ρ is the density. From the evolutionary equation of the scale factor a :

$$\frac{\ddot{a}}{a} = -\frac{1}{2}(1 + 3w)\frac{\dot{a}^2}{a^2} \quad (1)$$

we can see that an accelerating Universe desires $w < -\frac{1}{3}$, which suggests that the pressure of dark energy is negative. Here we use the units that $8\pi G = 1$. With the equation of state $w = -1$, the cosmological constant Λ has provided a good description for the accelerating Universe. However, since the quantum vacuum energy plays the same role as the cosmological constant, one cannot explain why the observed cosmological constant is so small. The value of vacuum energy density contributed from the sum of all vacuum modes below an ultraviolet cut-off at the Planck scale is given by $\rho_\Lambda \sim 10^{12}\text{erg/cm}^3$, which exceeds the observational value of $\rho_\Lambda \sim 10^{-8}\text{erg/cm}^3$ by about 120 orders of magnitude[8].

Therefore, different dark energy models other than the cosmological constant have been suggested to describe the accelerating Universe. Among the models, the scalar field models of dark energy may probe the nature of the acceleration of the Universe. Such a kind of scalar field is called quintessence[9, 10], which is considered as one of the candidates of dark energy that inspired by quantum theory. R.Caldwell suggested another type of scalar field in the Universe named phantom[11, 12]. In Ref.[13–16], the authors pointed out that the big rip in late Universe of phantom dark energy can be avoided. With $w < -1$ more generalized dynamical models of dark energy like quintom [17], k-essence[18] and H-essence[19] are also widely discussed.

One way to generalize the phantom Universe is to consider the imperfect fluid. The evolution of imperfect fluid is a dissipative process, which can be described by bulk viscosity, shear viscosity and heat conduction. The viscous relativistic fluids were first suggested in Refs.[20, 21]. In the general theory of dissipation in relativistic imperfect fluid, the evolution equation becomes very complicated. Fortunately, if we study the phenomenon in the quasi-thermal equilibrium state, the conventional theory is still valid. In fact, in the homogeneous and isotropic Universe,

*Electronic address: wjykana@foxmail.com

†Electronic address: fengcj@shnu.edu.cn

‡Electronic address: zhaixh@shnu.edu.cn

§Electronic address: kychz@shnu.edu.cn

the dissipative processes can be described by bulk viscosity and the shear viscosity can be ignored. The bulk viscosity introduces dissipation by re-defining the effective pressure p_{eff} as

$$p_{eff} = p_i - 3\xi_i H, \quad (2)$$

where ξ_i is the bulk viscosity coefficient of any component and H is the Hubble parameter. Up to now, how dissipative processes may affect the evolution of Universe has been conscientiously studied[22–36]. It is found that the viscosity plays an important role in the evolution of the Universe. For example, in Ref.[22], the author studied the cosmological dynamics of the viscous generalized Chaplygin gas, giving the constraints of the parameters. In Ref.[31], the author discussed the viscous Cardassian models and fit the models with Ia SN data, which is instructive in the study of observational cosmology. The authors of Ref.[32] alleviated the cosmological age problem by investigating the viscous Ricci dark energy. And in Ref.[27] do a statistics analysis considering an interacting and viscous Universe and perform a dynamics system approach as well. For this paper, we investigate the viscous phantom Universe by assuming that there is bulk viscosity in the phantom dark energy.

On the other hand, the dynamic system of the Universe is a non-linear system so it is hard to find its analytic solution. In order to describe the evolution of a dynamical system, people usually find the critical points of the system and study the perturbations around these critical points to determine the stability of the system. Another advantage of the dynamical approach is that it can completely avoid the influence of non-linear effect. Thus, in the study of cosmology, the dynamical method is widely used in the discussions of dark energy[37] or modified gravitation[38]. General reviews of the autonomous systems in FLRW universe have been given in Refs.[39, 40].

In this paper, we will assume the existence of the bulk viscosity in the phantom dark energy and investigate the evolution of the viscous phantom Universe by the dynamical approach. The paper is organized as follows. In Sec.II we give a brief review on the phantom dark energy and reconstruct the viscous phantom models. We study three different models of viscous phantom dark energy respectively in Sec.III, Sec.IV and Sec.V respectively. Among the three models, Model C is a special case with tracking attractor. Finally, discussions and conclusions will be given in Sec.VII.

II. VISCIOUS PHANTOM DARK ENERGY

The Friedman-Lemaitre-Robertson-Walker (FLRW) metric that describes a homogeneous and isotropic flat Universe is given by

$$ds^2 = -dt^2 + a(t)^2 \left[dr^2 + r^2(d\theta^2 + \sin^2\theta d\phi^2) \right], \quad (3)$$

where $a(t)$ is the scale factor.

The action of the phantom field reads as

$$S = \int d^4x \sqrt{-g} \left[\frac{1}{2} R - (\partial\phi)^2 + V(\phi) \right] + S_m. \quad (4)$$

The Friedmann equations of the Universe composed by dust matter and phantom field reads

$$H^2 = \frac{1}{3} (\rho_m + \rho_\phi), \quad (5)$$

$$\dot{H} = -\frac{1}{2} (\rho_m + \rho_\phi + p_\phi), \quad (6)$$

where ρ_i and p_i are the density and pressure of different components.

The dissipation of bulk viscosity is introduced by the effective pressure of phantom field[20, 22, 31, 32]

$$p_{eff} = p_\phi - 3\xi_\phi H, \quad (7)$$

and the evolutionary equation of phantom field can be written as

$$\ddot{\phi} + 3H\dot{\phi} - \frac{dV(\phi)}{d\phi} + \frac{9\xi_\phi H^2}{\dot{\phi}} = 0, \quad (8)$$

where ξ_ϕ is the bulk viscosity coefficient of phantom field. Due to the second law of thermodynamics, we have $\xi_\phi > 0$ that assures a positive entropy production. So the evolution equations for the dust matter and the phantom fields can be written as

$$\dot{\rho}_m + 3H\rho_m = 0, \quad (9)$$

$$\dot{\rho}_\phi + 3H(\rho_\phi + p_\phi - 3H\xi_\phi) = 0. \quad (10)$$

We introduce the dimensionless variables as follows:

$$\begin{aligned} x &= \frac{\dot{\phi}}{\sqrt{6}H}, & y &= \frac{\sqrt{V(\phi)}}{\sqrt{3}H}, \\ \lambda &= -\frac{V'(\phi)}{V(\phi)}, & \Gamma &= \frac{V(\phi)V''(\phi)}{V'(\phi)^2}, & \zeta &= \frac{\xi_\phi}{3H}. \end{aligned} \quad (11)$$

The relative densities of the components are given by

$$\Omega_m = 1 + x^2 - y^2, \quad (12)$$

$$\Omega_\phi = -x^2 + y^2. \quad (13)$$

And the EoS of phantom field reads

$$w_\phi = \frac{p_\phi}{\rho_\phi} = \frac{-x^2 - y^2 - \frac{\xi_\phi}{H}}{-x^2 + y^2}. \quad (14)$$

We may obtain

$$w_{eff} = -1 - \frac{2}{3} \frac{\dot{H}}{H^2}, \quad (15)$$

$$\dot{H}/H^2 = -\frac{3}{2} \left(1 - x^2 - y^2 + \frac{\xi_\phi}{3H} \right). \quad (16)$$

For viscous phantom cosmological dynamical system, the equations of autonomous system can be expressed as

$$\frac{dx}{dN} = -3x - \frac{\sqrt{6}}{2}\lambda y^2 + \frac{3}{2}x \left[1 - x^2 - y^2 - \zeta \right] - 3\zeta, \quad (17)$$

$$\frac{dy}{dN} = -\frac{\sqrt{6}}{2}\lambda xy + \frac{3}{2}y \left[1 - x^2 - y^2 - \zeta \right], \quad (18)$$

$$\frac{d\lambda}{dN} = -\sqrt{6}\lambda^2 x (\Gamma - 1). \quad (19)$$

$$(20)$$

where $N = \ln a = -\ln(1+z)$. We will study three models with differnt viscosity in the following sections.

III. AUTONOMOUS SYSTEM OF MODEL A: $\xi_\phi = 3\xi_0 H$

Firstly we are interested in the model whose bulk viscosity proportional to the Hubble parameter, given by $\xi_\phi = 3\xi_0 H$. In this model, we choose the exponential potential as

$$V(\phi) = V_0 e^{-\alpha\phi}, \quad (21)$$

where α and V_0 are positive constants. Thus, the equations of dynamical system of Model A can be reduced as the following equations:

$$\frac{dx}{dN} = -3x - \frac{\sqrt{6}}{2}\alpha y^2 + \frac{3}{2}x \left[1 - x^2 - y^2 - \xi_0 \right] - 3\xi_0, \quad (22)$$

$$\frac{dy}{dN} = -\frac{\sqrt{6}}{2}\alpha xy + \frac{3}{2}y \left[1 - x^2 - y^2 - \xi_0 \right], \quad (23)$$

from which the critical points are obtained and the physical conditions of these critical points can be studied, See Table I. And we may also perform perturbations to study the stability of these points by substituting linear perturbations near the critical points in the form as

$$x = x_{(Ai)} + \delta x, \quad (24)$$

$$y = y_{(Ai)} + \delta y, \quad i \in (1, 2), \quad (25)$$

where $x_{(Ai)}$ and $y_{(Ai)}$ denote the coordinates of the critical points $(x_{(Ai)}, y_{(Ai)})$. From the perturbation equations

$$\frac{d}{dN} \begin{pmatrix} \delta x \\ \delta y \end{pmatrix} = \begin{pmatrix} -\frac{3}{2}(1 + 3x^2 + y^2 + \xi_0) & -3xy - \sqrt{6}\alpha y \\ -3xy - \sqrt{\frac{3}{2}}\alpha y & \frac{1}{2}(3 - 3x^2 - 9y^2 - \sqrt{6}\alpha x - \xi_0) \end{pmatrix} \begin{pmatrix} \delta x \\ \delta y \end{pmatrix}, \quad (26)$$

we may give the eigenvalues of each point. For a 2D autonomous system, a stable point requires the real part of both eigenvalues to be negative, a saddle point is with one eigenvalue having a real part and the other having a negative one, and the point is unstable if the real parts of both eigenvalues are positive. Ignoring the unphysical points, we list the two fixed points of the autonomous equations in Table I, labelled as Case (A1) and Case (A2).

Case	Critical points (x, y)	Physical Conditions	Stable Condition	Stability
(A1)	$(x_{(A1)}, 0)$	$\xi_0 < 2$	$(\alpha, \xi_0) \in \text{I}$	Stable
			$(\alpha, \xi_0) \in \text{II}$	Saddle
			$(\alpha, \xi_0) \in \text{III}$	Unstable
(A2)	$(x_{(A2)}, y_{(A2)})$	$\xi_0 < \frac{1}{12} \left(-3 + \sqrt{6}\alpha + \sqrt{6\alpha^2 - 6\sqrt{6} + 81} \right)$	$(\alpha, \xi_0) \in \text{I}$	Stable
			$(\alpha, \xi_0) \in \text{II}$	Saddle

$$x_{(A1)} = -\frac{1+\xi_0}{3^{1/3}} \Lambda_A + (9^{1/3} \Lambda_A)^{-1}, \quad \Lambda_A = (-9\xi_0 + \sqrt{3}\sqrt{\xi_0^3 + 30\xi_0^2 + 3\xi_0 + 1})^{-1/3}.$$

$$x_{(A2)} = \frac{-\alpha^2 + 3 - \Delta_A}{2\sqrt{6}\alpha}, \quad y_{(A2)} = \sqrt{1 - \frac{\sqrt{6}}{3}\alpha x_{(A2)} - \xi_0 - x_{(A2)}^2}.$$

$$\Delta_A = \sqrt{\alpha^4 + 6\alpha^2 - 12\alpha^2\xi_0 + 12\sqrt{6}\alpha\xi_0 + 9}.$$

TABLE I: The fixed points and their stability of autonomous system of Model A.

For Case (A1), the eigenvalues of the perturbation matrix are given by

$$\lambda_1 = -\frac{3}{2}(1 + 3x_{A1}^2 + \xi_0), \quad (27)$$

$$\lambda_2 = \frac{1}{2}(3 - 3x_{A1}^2 - \sqrt{6}\alpha x_{A1} - \xi_0), \quad (28)$$

It is conceivable that the stability of this critical point is determined by the values of α and ξ_0 . The corresponding regions of the two parameters to the stability are shown in Fig I(a) and also listed in Table I. This point trends to $(0, 0)$ when $\xi_0 \rightarrow 0$, thus it represent a matter dominated Universe.

Case (A2) is the only non-trivial critical point besides case (A1), which represents a phantom dominated Universe. The eigenvalues of the perturbation matrix are given by

$$\lambda_3 = \frac{1}{4} \left[C_1 x_{A2} + C_2 - \sqrt{D_1 x_{A2}^3 + D_2 x_{A2}^2 + D_3 x_{A2} + D_4} \right], \quad (29)$$

$$\lambda_4 = \frac{1}{4} \left[C_1 x_{A2} + C_2 + \sqrt{D_1 x_{A2}^3 + D_2 x_{A2}^2 + D_3 x_{A2} + D_4} \right]. \quad (30)$$

where C_1, C_2 and D_1 to D_4 are coefficient composed of α and ξ_0 (see Appendix A). The regions of α and ξ_0 indicating the stability of the critical points (A_2) are illustrated in Fig.1(b) and the stable area of (A1) and (A2) are separate. However, in a physical view, we want α and ξ_0 to be small. So in the following study we may consider case (A1) as a saddle point and case (A2) as a stable point. The phase diagrams are also given in the figures below.

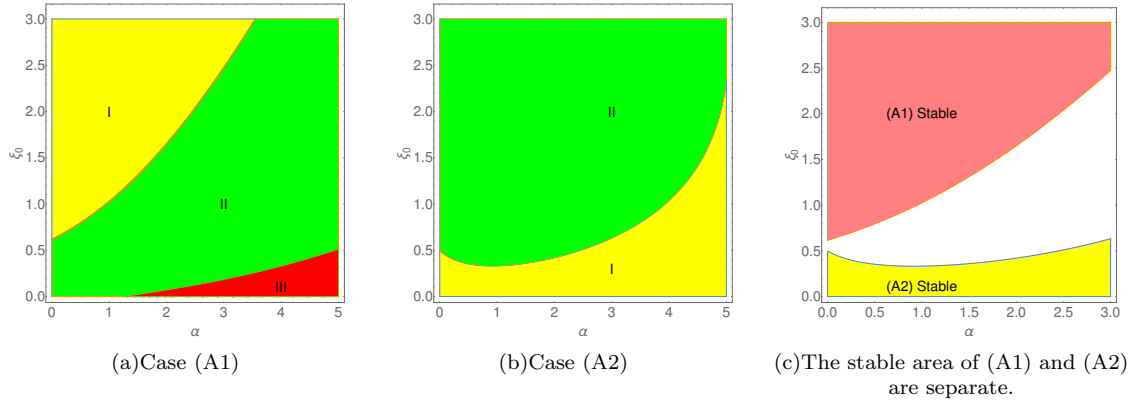


FIG. 1: The stable region of Case (A1) and Case (A2). In Figure.(a), the yellow region named "I" is the stable region of Case (A1). Similarly the green region named "II" is saddle region and the red one named "III" is unstable region. The stable condition of Case (A2) is shown in Figure.(b), the yellow region named "I" is the stable region and green region named "II" is saddle region. In Figure.(c), the upper pink region is the stable region for Case (A1) and the lower yellow region is the stable region for Case (A2). It is clearly shown that the stable region of the two fixed points separate from each other.

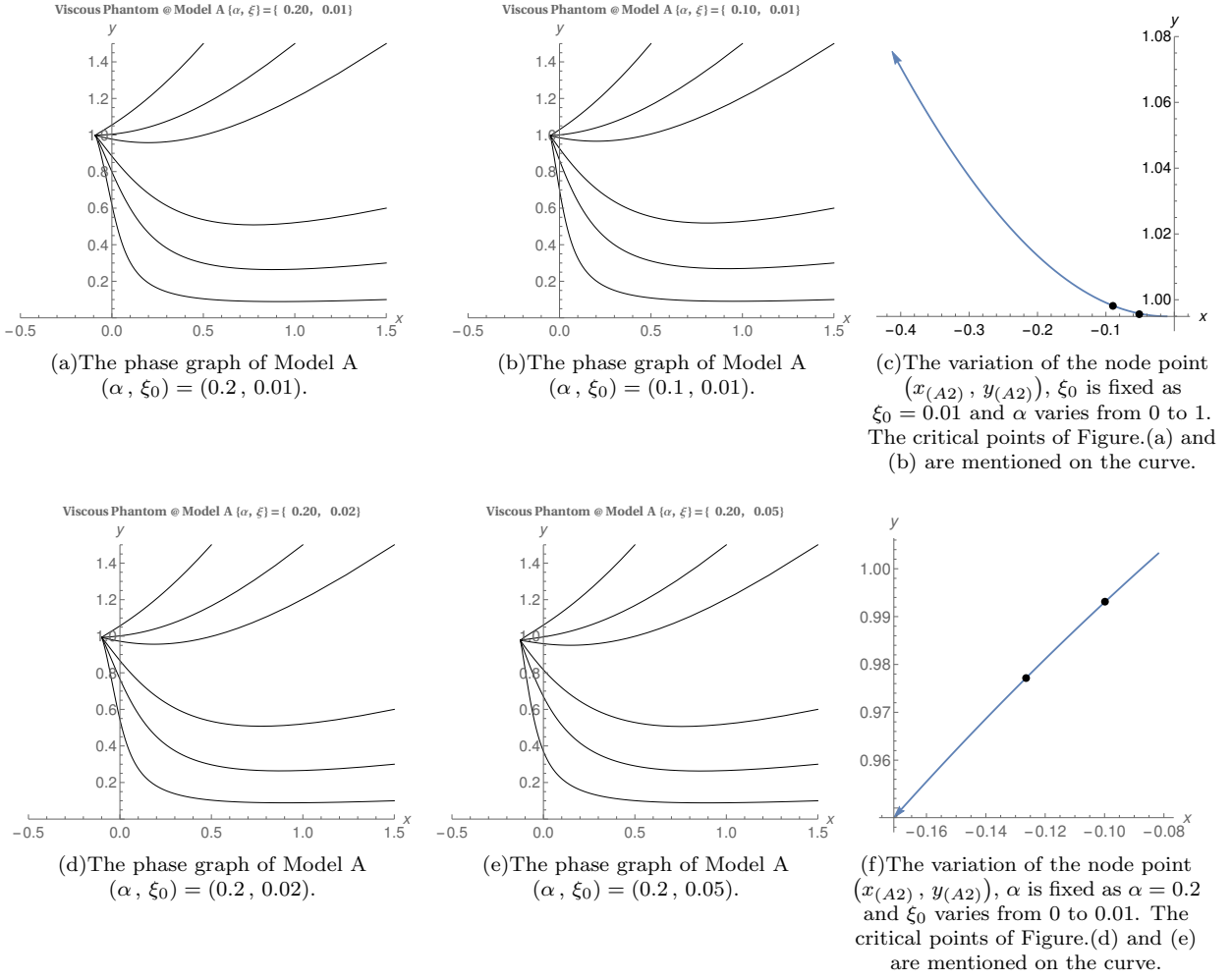


FIG. 2: The phase graph of the Model A for different initial of x and y . In Figure (a), (b) and (c), we have set that $\xi_0 = 0.01$. $\alpha = 0.2$ in Figure (a) and $\alpha = 0.1$ for Figure (b). In Figure (c) we enlarge the figure and show how the node point varies with α , from $\alpha = 0$ to $\alpha = 1$. The critical point of figure(a) and figure(b) are specially mentioned on the curve. Similarly, in Figure (d), (e) and (f), we set $\alpha = 0.2$ with variable ξ_0 and in Figure (f) we enlarge the figure and show how the spiral point varies with ξ_0 , from $\xi_0 = 0$ to $\xi_0 = 0.01$.

IV. AUTONOMOUS SYSTEM OF MODEL B: $\xi_\phi = \xi_0 \dot{\phi}$

Another form for bulk viscosity that we are interested in is $\xi_\phi = \xi_0 \dot{\phi}$. The equations of dynamical system of Model B could be reduced to the following equations:

$$\frac{dx}{dN} = -3x - \frac{\sqrt{6}}{2}\alpha y^2 + \frac{3}{2}x \left[1 - x^2 - y^2 - \xi_0 x \right] - 3\xi_0 x, \quad (31)$$

$$\frac{dy}{dN} = -\frac{\sqrt{6}}{2}\alpha xy + \frac{3}{2}y \left[1 - x^2 - y^2 - \xi_0 x \right]. \quad (32)$$

Similar to Model A, the critical points for the dynamical system are listed in Table.II.

Case	Critical points (x, y)	Stability
(B1)	$(0, 0)$	Saddle
(B2)	$(x_{(B2)}, y_{(B2)})$	Stable

$$x_{(B2)} = \frac{1}{4\sqrt{6}\alpha} \left[6 - 2\alpha^2 - \sqrt{6}\alpha\xi_0 + 6\xi_0 - \sqrt{(6 - 2\alpha^2 - \sqrt{6}\alpha\xi_0 + 6\xi_0)^2 + 48\alpha^2} \right].$$

$$y_{(B2)} = \frac{1}{3} \left(3x_{(B2)}^2 + (\sqrt{6}\alpha + 3\xi_0)x_{(B2)} - 3 \right).$$

TABLE II: The fixed points and their stability of autonomous system of Model B.

In Model B, case (B2) remain positive when $\alpha > 0$ and $\xi_0 > 0$, see details in Appendix B. Next, we study the above model numerically. The initial values of x and y are chosen as shown in Fig.4.

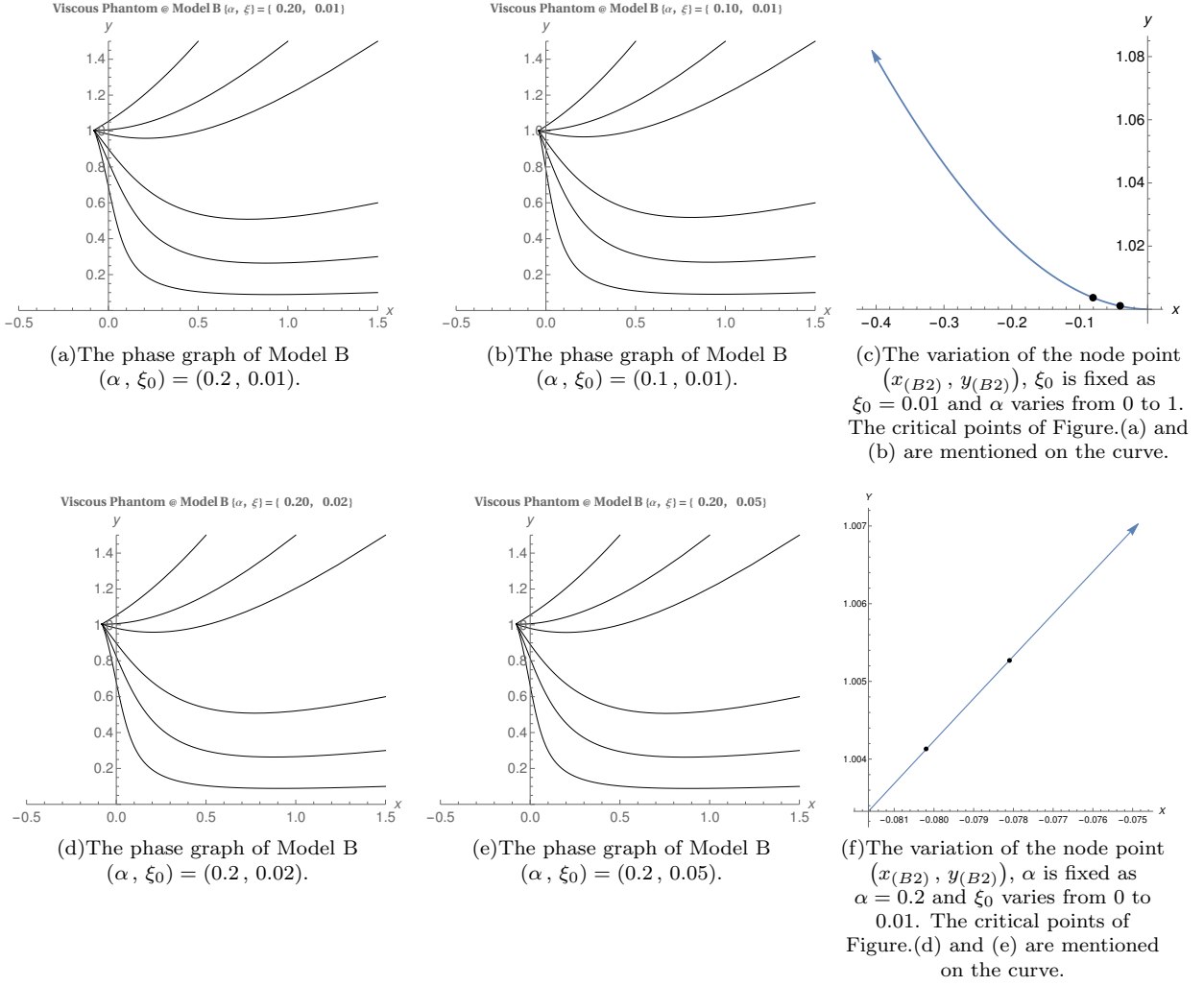


FIG. 3: The phase graph of the Model B for different initial of x and y . In Figure (a), (b) and (c), we have set that $\xi_0 = 0.01$. $\alpha = 0.2$ in Figure (a) and $\alpha = 0.1$ for Figure (b). In Figure (c) we enlarge the figure and show how the node point varies with α , from $\alpha = 0$ to $\alpha = 1$. The critical point of figure(a) and figure(b) are specially mentioned on the curve. Similarly, in Figure (d), (e) and (f), we set $\alpha = 0.2$ with variable ξ_0 and in Figure (f) we enlarge the figure and show how the spiral point varies with ξ_0 , from $\xi_0 = 0$ to $\xi_0 = 0.1$.

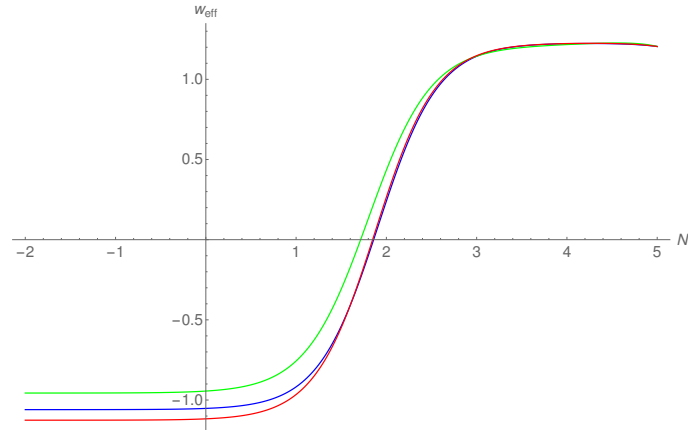


FIG. 4: The lower red line and blue line the evolution of the equation of state w_{eff} of Model A and Model B but the same initial values of x and y separately. We choose the parameters as $(\alpha, \xi_0) = (0.2, 0, 01)$ in the figure. And the upper green line is the equation of state w_{eff} of Model A but the parameters as are chosen as $(\alpha, \xi_0) = (0.2, 0, 05)$.

V. AUTONOMOUS SYSTEM OF MODEL C: LARGE λ

Next, we study a special model to see the tracking behavior of viscous phantom dark energy. Supposing that λ is very large and Γ is nearly constant but is not 1, we make the following transformation similar with literature[14, 41, 42].

$$\begin{aligned}\epsilon &= \frac{1}{\lambda}, \\ x &= \epsilon X, \\ y &= \epsilon Y, \\ \xi_\phi &= \epsilon \xi.\end{aligned}\tag{33}$$

We also suppose that ξ is nearly constant. The terms with ϵ omitted, the autonomous system can be rewritten in terms of new variables X and Y as:

$$\frac{dX}{dN} = -\frac{3}{2}X - \frac{\sqrt{6}}{2}Y^2 - 3\xi - \sqrt{6}(\Gamma - 1)X^2,\tag{34}$$

$$\frac{dY}{dN} = \frac{3}{2}Y - \frac{\sqrt{6}}{2}XY - \sqrt{6}(\Gamma - 1)XY.\tag{35}$$

Thus, we may obtain the non-trivial and physical allowed point among the critical points:

$$(X_c, Y_c) = \left(\frac{3}{2}\Gamma_a, \frac{\Gamma_a}{\sqrt{2}} \sqrt{\frac{-2\sqrt{6}\xi}{\Gamma_a^2} - \frac{6}{\Gamma_a} + 3} \right)\tag{36}$$

where $\Gamma_a = \frac{1}{2\Gamma-1}$. At this state, the corresponding energy density parameter of viscous phantom field is given by

$$\Omega_{DE} = -\frac{3}{2}\Gamma_a + \frac{\Gamma_a}{\sqrt{2}} \sqrt{\frac{-2\sqrt{6}\xi}{\Gamma_a^2} - \frac{6}{\Gamma_a} + 3}.\tag{37}$$

And the EoS of viscous phantom energy read as

$$w_{DE} = \frac{-\frac{3}{2}\Gamma_a - \frac{\Gamma_a}{\sqrt{2}} \sqrt{\frac{-2\sqrt{6}\xi}{\Gamma_a^2} - \frac{6}{\Gamma_a} + 3} - \xi}{-\frac{3}{2}\Gamma_a + \frac{\Gamma_a}{\sqrt{2}} \sqrt{\frac{-2\sqrt{6}\xi}{\Gamma_a^2} - \frac{6}{\Gamma_a} + 3}}.\tag{38}$$

From the physical requirement $0 \leq \Omega_{DE} \leq 1$, the viable area of Γ and ξ is shown in the Fig.5 below.

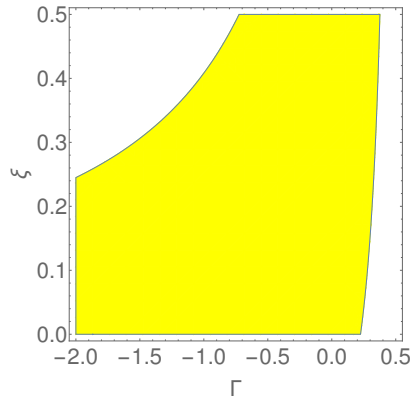


FIG. 5: The viable area of Γ and ξ in Model C

As remarked before, λ is large, thus we can easily find that the critical point (X_c, Y_c) lead to a matter dominated Universe. And the density parameter of the viscous phantom field would track with the evolution of dark matter.

Next we will study the stability of the critical point. Similar to Model A and Model B, we have

$$\frac{d\delta X}{dN} = \left[-\frac{3}{2} - 2\sqrt{6}X(\Gamma - 1) \right] \delta X - \sqrt{6}Y\delta Y, \quad (39)$$

$$\frac{d\delta Y}{dN} = -\sqrt{\frac{3}{2}}\frac{Y}{\Gamma_a}\delta X + \frac{1}{2}\left(3 - \frac{\sqrt{6}X}{\Gamma_a}\right)\delta Y. \quad (40)$$

The eigenvalues are given by

$$\Lambda_1 = 4\Gamma_a \left(-9\Gamma_a + 6 - \sqrt{3}\sqrt{\Delta_c} \right), \quad (41)$$

$$\Lambda_2 = 4\Gamma_a \left(-9\Gamma_a + 6 + \sqrt{3}\sqrt{\Delta_c} \right), \quad (42)$$

where

$$\Delta_c = -128\sqrt{6}\Gamma^3\xi + 192\sqrt{6}\Gamma^2\xi - 84\Gamma^2 - 96\sqrt{6}\Gamma\xi + 60\Gamma + 16\sqrt{6}\xi + 3. \quad (43)$$

According to the previous discussion, we found that in the viable area of (Γ, ξ) the eigenvalues are negative. Thus this is a stable point.

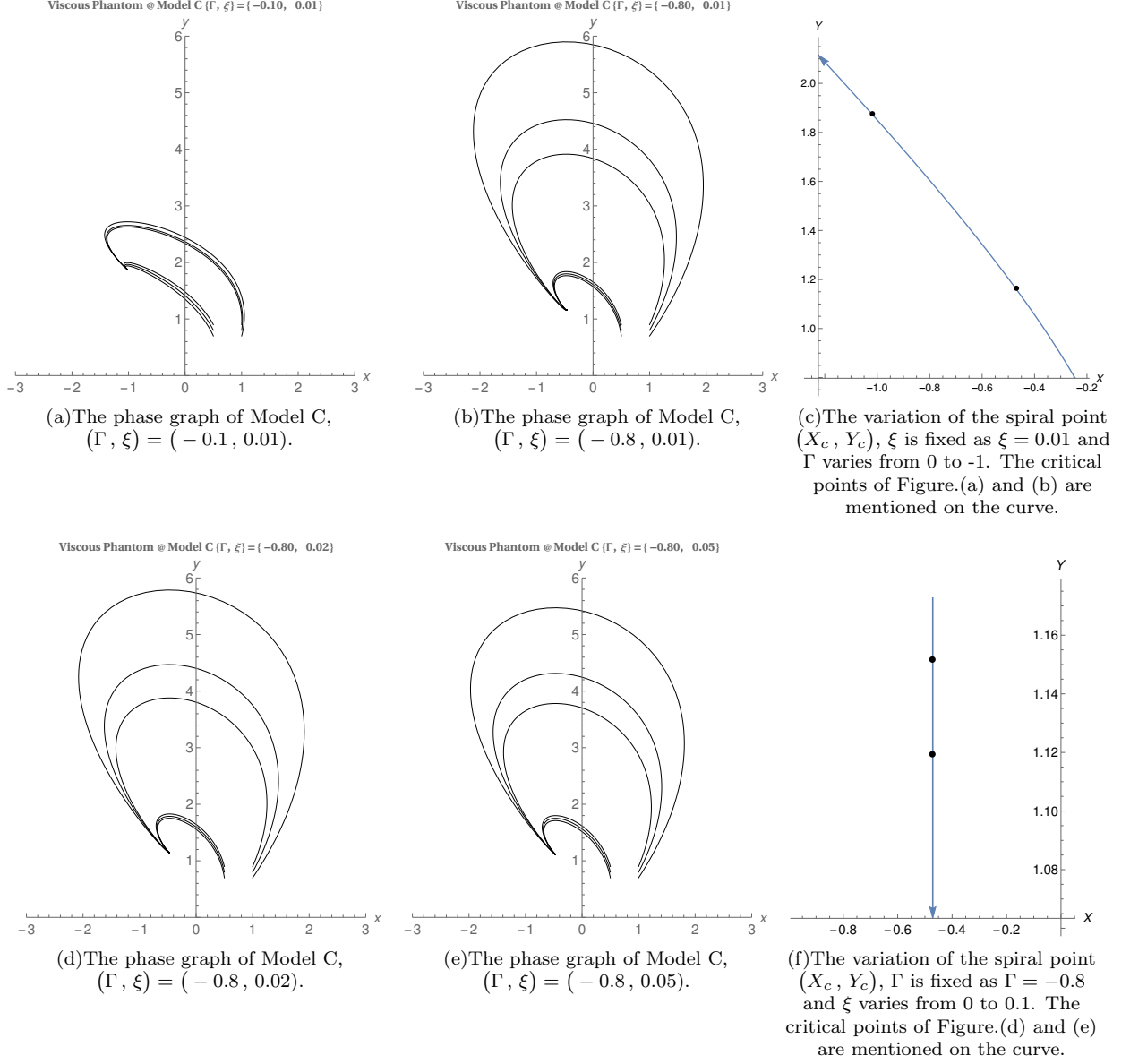


FIG. 6: The phase graph of the Model C for different initial X and Y . We have set that $\xi_0 = 0.01$ in these figures. $\Gamma = -0.1$ in Figure (a) and $\Gamma = -0.8$ for Figure (b). In Figure (c) we show how the spiral point varies with Γ , from $\Gamma = 0$ to $\Gamma = -1$. The critical point of figure(a) and figure(b) are specially mentioned on the curve. Similarly, in Figure (d), (e) and (f), we set $\Gamma = -0.8$ with variable ξ and in Figure (f) we enlarge the figure and show how the spiral point varies with ξ_0 , from $\xi = 0$ to $\xi = 0.1$.

VI. EXAMPLE OF TRACKING SOLUTION OF VISCOUS PHANTOM DARK ENERGY

Next we may show a special potential function that may lead to a tracking solution. The equation of motion of viscous phantom field can be rewritten as

$$\ddot{\phi} + 3H\dot{\phi} + \frac{dU(\phi)}{d\phi} = 0, \quad (44)$$

where

$$\frac{dU(\phi)}{d\phi} = -\frac{dV(\phi)}{d\phi} + \frac{9\xi_\phi H^2}{\dot{\phi}}. \quad (45)$$

And we choose the viscosity that

$$\xi_\phi = \frac{\xi_0 \dot{\phi}}{H^2}. \quad (46)$$

According to literature[43], the potential function of the scalar field with a tracking solution is given by

$$U(\phi) = \frac{1-w_\phi}{2} \rho_{\phi 0} \left[\sqrt{\frac{\Omega_{m0}}{\Omega_{\phi 0}}} \sinh\left(\frac{3(w-w_\phi)}{2\sqrt{-3(1+w_\phi)}}(\phi-\phi_{in})\right) \right]^{-2(1+w_\phi)/(w-w_\phi)}, \quad (47)$$

where $w \neq w_\phi$ and ϕ_{in} is a constant depending on the initial condition. Thus, the potential function of the viscous phantom field is given by

$$V(\phi) = -\frac{1-w_\phi}{2} \rho_{\phi 0} \left[\sqrt{\frac{\Omega_{m0}}{\Omega_{\phi 0}}} \sinh\left(\frac{3(w-w_\phi)}{2\sqrt{-3(1+w_\phi)}}(\phi-\phi_{in})\right) \right]^{-2(1+w_\phi)/(w-w_\phi)} + 9\xi_0(\Omega_{m0} - \Omega_{\phi 0}) + V_1. \quad (48)$$

Here we have put the viscous term into the potential term and w_ϕ is given by Eq.(14). V_1 is an integration constant. Specially, when matter dominants and $\Omega_m \gg \Omega_\phi$, the potential function turns to

$$V(\phi) = -\frac{1-w_\phi}{2} \rho_{\phi 0} \left[\sqrt{\frac{\Omega_{m0}}{-3(1+w_\phi)\Omega_{\phi 0}}} \frac{3(w-w_\phi)}{2}(\phi-\phi_{in}) \right]^{2(1+w_\phi)/(w_\phi-w)} + 9\xi_0\Omega_{m0} + V_1. \quad (49)$$

VII. CONCLUSION AND DISCUSSION

In this paper, the cosmological dynamics of viscous phantom Universe is investigated qualitatively and numerically. The three types of viscosity are listed here:

- (1) Model A: $\xi_\phi = 3\xi_0 H$,
- (2) Model B: $\xi_\phi = \xi_0 \dot{\phi}$,
- (3) Model C: Big λ .

In the above discussion, we have analyzed the dynamical evolution field for viscous phantom or different parameters and initial conditions. We find that there are two critical points that describe a late time transition from matter dominated era to phantom dominated one in Model A and Model B. Since the potential function $V(\phi)$ are both $V_0 e^{-\alpha\phi}$ in Model A and Model B, we find that with the increase of the value of α , the node point moves away from the point (0, 1). However, in Model A, when α is fixed, if the viscosity is big enough, the critical point may move into the regime that $-\frac{1}{3} < w_{eff} < -1$, which means the viscosity does play an important role in the evolution of the Universe. The dynamical approach of Model A and Model B also place constraints on the parameters in the exponential potential. We have also discussed the dynamics of the viscous phantom field for a general potential and reach the tracking solution in some special cases.

After all, due to its ability to produce observational predictions cosmology is always a testable theory and we believe that in the future some new experiments with multiple observations and techniques will improve our knowledge of late-time accelerating expansion. For example, in Ref.[44], demonstrated that quintessence dark energy models can be ruled out in the next 5 years independently of cosmological observations if long-baseline neutrino experiments measure the neutrino mass ordering to be inverted. And the development of artificial neural network [45] may help in the future study.

Acknowledgments

This work is supported by National Science Foundation of China grant Nos. 11105091 and 11047138, ‘‘Chen Guang’’ project supported by Shanghai Municipal Education Commission and Shanghai Education Development Foundation Grant No. 12CG51, and Shanghai Natural Science Foundation, China grant No. 10ZR1422000. The authors would like to thank Ping Xi for the useful discussions.

Appendix A: The Dynamics of Model A

In this appendix ,we may give a brief discussion for the dynamics of Model A.

$$-3x - \frac{\sqrt{6}}{2}\alpha y^2 + \frac{3}{2}x \left[1 - x^2 - y^2 - \xi_0 \right] - 3\xi_0 = 0, \quad (\text{A1})$$

$$-\frac{\sqrt{6}}{2}\alpha xy + \frac{3}{2}y \left[1 - x^2 - y^2 - \xi_0 \right] = 0. \quad (\text{A2})$$

When y is zero, we can obtain that

$$x^3 + (1 + \xi_0)x + 2\xi_0 = 0. \quad (\text{A3})$$

This is a linear equation with stardard form that we easily can solve it by Cardan formula:

$$-3x + \frac{3}{2}x \left[1 - x^2 - \xi_0 \right] - 3\xi_0 = 0. \quad (\text{A4})$$

Thus we may obtain the Case (A1) after ignoring the complex solutions.

When y is not zero, we can obtain that

$$0 = 2\sqrt{6}\alpha x^2 + 2(\alpha^2 - 3)x + \sqrt{6}(\xi_0 - 1) - 6\xi_0, \quad (\text{A5})$$

$$y^2 = 1 - \frac{\sqrt{6}}{3}\alpha x - \xi_0 - x^2. \quad (\text{A6})$$

And we want a physical solution that observe $0 < -x^2 + y^2 < 1$ when α and ξ_0 are positive. Thus, this viable critical point is listed in Table I.

Next we may discuss the eigenvalues of the two points.

For case (A1), y is zero, the perturbation matrix is given by

$$M_1 = \begin{pmatrix} -\frac{3}{2}(1 + 3x^2 + \xi_0) & 0 \\ 0 & \frac{1}{2}(3 - 3x^2 - 9y^2 - \sqrt{6}\alpha x - \xi_0) \end{pmatrix}. \quad (\text{A7})$$

The eigenvalues observe the equation

$$\lambda^2 - \text{Tr}M_1\lambda + \text{Det}M_1 = 0. \quad (\text{A8})$$

So we can obtain

$$\lambda_1 = -\frac{3}{2}(1 + 3x^2 + \xi_0). \quad (\text{A9})$$

$$\lambda_2 = \frac{1}{2}(3 - 3x^2 - 9y^2 - \sqrt{6}\alpha x - \xi_0). \quad (\text{A10})$$

When y is not zero, the eigenvalues are given by

$$\lambda_3 = \frac{1}{4} \left[C_1x + C_2 - \sqrt{D_1x^3 + D_2x^2 + D_3x + D_4} \right], \quad (\text{A11})$$

$$\lambda_4 = \frac{1}{4} \left[C_1x + C_2 + \sqrt{D_1x^3 + D_2x^2 + D_3x + D_4} \right]. \quad (\text{A12})$$

where

$$C_1 = 3\sqrt{6}\alpha, \quad (\text{A13})$$

$$C_2 = 6\xi_0 - 12, \quad (\text{A14})$$

$$D_1 = -96\sqrt{6}\alpha, \quad (\text{A15})$$

$$D_2 = 2(-93\alpha^2 + 72), \quad (\text{A16})$$

$$D_3 = -4\sqrt{6}\alpha(4\alpha^2 + 15\xi_0 - 13), \quad (\text{A17})$$

$$D_4 = -48\alpha^2(\xi_0 - 1) + 36\xi_0^2. \quad (\text{A18})$$

With the results one can discuss the stability of the model.

Appendix B: Dynamic System of Model B

Similar to Model A, in Model B, the trace and determinant of the perturbation matrix are given by

$$\text{Tr}M_2 = \frac{3}{2}x(\sqrt{6}\alpha + \xi_0) - 3(2 + \xi_0), \quad (\text{B1})$$

$$\text{Det}M_2 = 6\sqrt{6}\alpha x^3 + \frac{3}{2} \left(10\alpha^2 + 5\sqrt{6}\alpha\xi_0 - 6(\xi_0 + 1) \right) x^2 \quad (\text{B2})$$

$$+ \left(\sqrt{6}\alpha^3 + 6\alpha^2\xi_0 + 3\sqrt{\frac{3}{2}}\alpha((\xi_0 - 2)\xi_0 - 6) - 9\xi_0(\xi_0 + 1) \right) x - 3\alpha^2 - 3\sqrt{\frac{3}{2}}\alpha\xi_0 + 9\xi_0 + 9, \quad (\text{B3})$$

respectively. For $\text{Tr}M_2 < 0$, it is easily to see that

$$x < \frac{2\xi_0 + 4}{\sqrt{6}\alpha + \xi_0}, \quad (\text{B4})$$

when α and ξ_0 are both positive. Obviously, we always have

$$x_{(B2)} = \frac{1}{4\sqrt{6}\alpha} \left[6 - 2\alpha^2 - \sqrt{6}\alpha\xi_0 + 6\xi_0 - \sqrt{(6 - 2\alpha^2 - \sqrt{6}\alpha\xi_0 + 6\xi_0)^2 + 48\alpha^2} \right] < \frac{2\xi_0 + 4}{\sqrt{6}\alpha + \xi_0}. \quad (\text{B5})$$

So the trace of perturbation matrix is negative for the critical point (B2). And we can read from the matrix that the determinant of perturbation matrix is positive at the same point. Thus, the eigenvalues for the fixed point are both negative and the fixed point is a stable point.

-
- [1] A. G. Riess *et al.* [Supernova Search Team], *Astron. J.* **116** (1998) 1009
 - [2] S. Perlmutter *et al.* [Supernova Cosmology Project Collaboration], *Astrophys. J.* **517** (1999) 565
 - [3] D. N. Spergel *et al.* [WMAP Collaboration], *Astrophys. J. Suppl.* **148** (2003) 175
 - [4] D. J. Eisenstein *et al.* [SDSS Collaboration], *Astrophys. J.* **633** (2005) 560
 - [5] M. Kowalski *et al.* [Supernova Cosmology Project Collaboration], *Astrophys. J.* **686** (2008) 749
 - [6] N. Aghanim *et al.* [Planck Collaboration], arXiv:1807.06209 [astro-ph.CO].
 - [7] G. Hinshaw *et al.* [WMAP Collaboration], *Astrophys. J. Suppl.* **208** (2013) 19
 - [8] S. Weinberg, astro-ph/0005265.
 - [9] P. J. E. Peebles and B. Ratra, *Astrophys. J.* **325** (1988) L17.
 - [10] B. Ratra and P. J. E. Peebles, *Phys. Rev. D* **37** (1988) 3406.
 - [11] R. R. Caldwell, *Phys. Lett. B* **545** (2002) 23
 - [12] R. R. Caldwell, M. Kamionkowski and N. N. Weinberg, *Phys. Rev. Lett.* **91** (2003) 071301
 - [13] X. Z. Li and J. G. Hao, *Phys. Rev. D* **69** (2004) 107303
 - [14] J. G. Hao and X. z. Li, *Phys. Rev. D* **70** (2004) 043529
 - [15] J. g. Hao and X. z. Li, *Phys. Rev. D* **67** (2003) 107303
 - [16] X. Z. Li, Y. B. Zhao and C. B. Sun, *Class. Quant. Grav.* **22** (2005) 3759
 - [17] Z. K. Guo, Y. S. Piao, X. M. Zhang and Y. Z. Zhang, *Phys. Lett. B* **608** (2005) 177
 - [18] A. D. Rendall, *Class. Quant. Grav.* **23** (2006) 1557
 - [19] H. Wei, R. G. Cai and D. F. Zeng, *Class. Quant. Grav.* **22** (2005) 3189
 - [20] C. Eckart, *Phys. Rev.* **58** (1940) 919.
 - [21] Landau, L D , and E. M. Lifshitz . 1959.
 - [22] X. H. Zhai, Y. D. Xu and X. Z. Li, *Int. J. Mod. Phys. D* **15** (2006) 1151
 - [23] I. H. Brevik, *Int. J. Mod. Phys. D* **15** (2006) 767
 - [24] S. Capozziello, V. F. Cardone, E. Elizalde, S. Nojiri and S. D. Odintsov, *Phys. Rev. D* **73** (2006) 043512
 - [25] S. Nojiri and S. D. Odintsov, *Phys. Rev. D* **72** (2005) 023003
 - [26] S. Nojiri and S. D. Odintsov, *Phys. Lett. B* **639** (2006) 144
 - [27] A. Hernandez-Almada, M. A. Garca-Aspeitia, J. Magaa and V. Motta, *Phys. Rev. D* **101** (2020) no.6, 063516
 - [28] I. Brevik, E. Elizalde, S. Nojiri and S. D. Odintsov, *Phys. Rev. D* **84** (2011) 103508
 - [29] I. Brevik, . Grn, J. de Haro, S. D. Odintsov and E. N. Saridakis, *Int. J. Mod. Phys. D* **26** (2017) no.14, 1730024
 - [30] B. D. Normann and I. Brevik, *Entropy* **18** (2016) 215
 - [31] C. B. Sun, J. L. Wang and X. Z. Li, *Int. J. Mod. Phys. D* **18** (2009) 1303
 - [32] C. J. Feng and X. Z. Li, *Phys. Lett. B* **680** (2009) 355
 - [33] M. G. Hu and X. H. Meng, *Phys. Lett. B* **635** (2006) 186

- [34] T. Koivisto and D. F. Mota, Phys. Rev. D **73** (2006) 083502
- [35] X. H. Meng, J. Ren and M. G. Hu, Commun. Theor. Phys. **47** (2007) 379
- [36] B. Pourhassan, Int. J. Mod. Phys. D **22** (2013) 1350061
- [37] C. J. Feng, X. Z. Li and P. Xi, JHEP **1205** (2012) 046
- [38] C. J. Feng, X. Z. Li and L. Y. Liu, Mod. Phys. Lett. A **29** (2014) no.07, 1450033
- [39] S. Bahamonde, C. G. Bhmer, S. Carloni, E. J. Copeland, W. Fang and N. Tamanini, Phys. Rept. **775-777** (2018) 1
- [40] E. J. Copeland, M. Sami and S. Tsujikawa, Int. J. Mod. Phys. D **15** (2006) 1753
- [41] S. C. C. Ng, N. J. Nunes and F. Rosati, Phys. Rev. D **64** (2001) 083510
- [42] P. J. Steinhardt, L. M. Wang and I. Zlatev, Phys. Rev. D **59** (1999) 123504 doi:10.1103/PhysRevD.59.123504
- [43] V. Sahni and A. A. Starobinsky, Int. J. Mod. Phys. D **9** (2000) 373
- [44] S. Vagnozzi, S. Dhawan, M. Gerbino, K. Freese, A. Goobar and O. Mena, Phys. Rev. D **98** (2018) no.8, 083501
- [45] Q. B. Cheng, C. J. Feng, X. H. Zhai and X. Z. Li, Phys. Rev. D **97** (2018) no.12, 123530